Pergamon

Int. J. Solids Structures Vol. 32, No. 8/9, pp. 1079–1097, 1995

0020-7683/95 $9.50 + .00

0020-7683(94)00184-7

ENDOCHRONIC EQUATIONS FOR FINITE PLASTIC DEFORMATION AND APPLICATION TO METAL TUBE UNDER TORSION

HAN C. WU, JUN K. LU† and WEN F. PAN‡
Department of Civil Engineering, The University of Iowa, Iowa City, IA 52242, U.S.A.

(*Received* 22 *October* 1992; *in revised form* 20 *July* 1994)

Abstract—Endochronic constitutive equations have been derived for use in the description of rigid-plastic deformation in the finite strain range. The concepts of corotational rate, corotational integral and plastic spin have been incorporated into the theory. The equations are then applied to describe the deformation of metal tubes subjected to torsion. Several different loading conditions have been considered. The theoretical results have been compared with the experimental data for three different metals. Reasonable agreement between theory and experiment has been achieved.

1. INTRODUCTION

The stress–strain behavior of materials subjected to finite plastic deformation has been a frequent subject of investigation in recent years. Significant progress has been made both from the phenomenological and physical approaches. In this work, the phenomenological approach is used by means of continuum mechanics and plasticity. It is believed that this approach has its merit in solving complex problems with relatively simple equations as compared to physical theories.

Most phenomenological theories are hinged on the concept of corotational rate. The Jaumann rate was generally used until the publication of Nagtegaal and De Jong (1981). These authors numerically evaluated the stress generated by simple shear using the Jaumann rate of back stress in a model that uses the Prager (1955) linear kinematic hardening rule. They found an oscillatory shear stress response to a monotonically increasing shear strain which is physically impossible. This result triggered a series of investigations to look for corotational stress rates appropriate for the description of metallic behavior in the finite strain range. The criterion for judgment has been to define a corotational rate in combination with a set of constitutive equations so that the shear stress response to a monotonically increasing shear strain is not oscillatory.

This goal has been achieved by several investigators using several different definitions of corotational rate. Some of the works are now cited. An earlier work of Dienes (1979) uses a corotational rate, based on the work of Green and Naghdi (1965), which is defined in terms of the rotation tensor from the polar decomposition of the deformation gradient. Lee *et al.* (1983) define the corotational rate by the spin of a unit vector which is oriented along a principal direction of the back stress. Sowerby and Chu (1984) assume that the corotational stress rate is defined by the stretch tensor decomposed from the deformation gradient. Dafalias (1984, 1985) defines the corotational rate by use of the plastic spin which was originally suggested by Mandel (1973) and Kratochvil (1973). The latter authors suggested that constitutive relations must be provided with a macroscopic formulation not only for the plastic rate of deformation but also for the plastic spin. Dafalias (1984, 1985) uses the representation theorem for isotropic functions to provide explicit forms of constitutive relation for the plastic spin. Aifantis (1987) chooses to compute the corotational rate with respect to the stress spin corresponding to the material frame whose angular

† Department of Civil Engineering, National Pingtong Polytechnic Institute, Taiwan.
‡ Department of Engineering Science, National Cheng Kung University, Taiwan.

velocity coincides with that of stress. Most investigations cited are based on the multiplicative decomposition by Lee (1969) who decomposed the deformation gradient tensor into the elastic and the plastic parts. Since the elastic strain (yield stress divided by the elastic modulus) is usually of the order of 10^{-3} for metals, it is small and frequently neglected.

Most theoretical investigators considered the case of loading only. Since information related to unloading and reloading is not generally available, these cases are rarely studied theoretically. However, they must be studied in order to verify a constitutive equation. It is known that the loading curve is not sensitive to various types of constitutive equations but the unloading curve is. Another area of concern is that most theoretical analyses consider two dimensional shearing, either simple or pure shear. However, experiments of two dimensional shearing are almost impossible to conduct and investigators have compared their theoretical results to results of torsion tests. It is our opinion that since the hoop stress is always zero in the torsion tests, this condition has to be enforced when the two dimensional shearing problems are solved and used to simulate the torsion tests. Thus, the boundary conditions of the material element of the theoretical analysis should be carefully considered, which has not been done, however, by most theoretical investigators.

The torsion test of a cylinder is a very convenient means of determining the strain-hardening characteristics of materials. However, it is not straightforward to determine the shear stress–strain curve from the experimental torque versus angle of twist data. This problem has been discussed by Wu *et al.* (1992). Other problems that we need to realize are that torsion of solid cylindrical specimens is useful only for loading without unloading; the axial effect depends significantly on the wall-thickness and gauge length of a tubular specimen; and that a short specimen does not give rise to uniform stress or strain in the gauge section. We need to consider these effects when the experimental results are used to compare with the theoretical results. Some experimental results that are used in this study are now cited. Swift (1947) tested several materials in pure torsion (shearing without constraint in the axial direction) and observed axial extension in relation to shear strain under cyclic loading. Bailey *et al.* (1972) tested 1100-aluminum in pure torsion and recorded the stress–strain relation together with the tangential (hoop) strain. Hart and Chang (1983) tested thin-walled tubes of purity nickel (Ni-200) in torsion with different amounts of axial prestress. White *et al.* (1990) tested specimens in simple shear state (shearing with axial ends fixed) and investigated the stress–strain response. Wu and Xu (1989, 1990) and Wu *et al.* (1993, 1994b) investigated the deformational behavior of aluminum and stainless steel subjected to torsion by use of long gaugelength specimens and an extensometer that they built.

The concept of plastic spin will be used in the present work. This concept of corotational rate with plastic spin was used by Im and Atluri (1987) in a version of endochronic theory to discuss finite deformation of metals. For an account of the endochronic theory of plasticity, see Valanis (1980) and Wu and Yip (1981). Im and Atluri (1987) derived the governing equations by using the isoclinic configuration as the intermediate configuration and the corresponding second Piola–Kirchhoff stress. In here, we obtain the governing equations by using the concepts of corotational integrals and derivatives discussed by Dafalias (1987). We use the Cauchy stress instead of the Kirchhoff stress used by Im and Atluri (1987). The use of the Cauchy stress is consistent with the finding of Wu *et al.* (1994a) that the evolution rule of yield surface is very complicated if stress measures such as the second Piola–Kirchhoff stress is used. We further express the plastic spin in terms of the back stress and the rate of deformation and show that the obtained expression is convenient in the applications considered. Even though the methods are different in the derivation, the resulting equations are similar to those of Im and Atluri (1987). However, the present derivation seems to be more straightforward. We also mention that Im and Atluri (1987) considered the loading condition only, while complex loading/unloading/reloading conditions are included in the present study. Our theoretical results will be compared with the aforementioned experimental results. In obtaining the theoretical results, we have enforced the requirement that the hoop stress be zero.

2. COROTATIONAL DERIVATIVES AND INTEGRALS

Suppose that a flexible body moves in space. The triad of unit vectors of frame $\bar{\underline{x}}$ that rotates with the body coincides with that of the reference frame $\underline{x}$ at time zero. The two sets of coordinates are related by

$$\bar{\underline{x}} = \underset{\sim}{M}^{T}\underline{x} \tag{1}$$

where $\underset{\sim}{M}$ is the matrix of an orthogonal tensor, such that $\underset{\sim}{M}^{T}\underset{\sim}{M} = \underset{\sim}{I}$.

Note that in this writing, a vector is denoted by a letter with an underscored bar, and a tensor is denoted by a letter with an underscored tilde. Then, the following transformation laws apply

$$\bar{\underline{g}} = \underset{\sim}{M}^{T}\underline{g}$$

$$\bar{\underset{\sim}{T}} = \underset{\sim}{M}^{T}\underset{\sim}{T}\underset{\sim}{M} \tag{2}$$

where $\bar{\underline{g}}$ and $\bar{\underset{\sim}{T}}$ refer to the $\bar{\underline{x}}$ frame and we may write the corotational derivatives for $\underline{g}$ and $\underset{\sim}{T}$ as

$$\overset{*}{\underline{g}} = \dot{\underline{g}} - \underset{\sim}{\Omega}\underline{g} \tag{3}$$

$$\overset{*}{\underset{\sim}{T}} = \dot{\underset{\sim}{T}} - \underset{\sim}{\Omega}\underset{\sim}{T} + \underset{\sim}{T}\underset{\sim}{\Omega} \tag{4}$$

where

$$\underset{\sim}{\Omega} = \dot{\underset{\sim}{M}}\underset{\sim}{M}^{T} \tag{5}$$

and a dot over a tensor denotes its material derivative. It is easy to show that

$$\overset{*}{\underset{\sim}{T}} = \underset{\sim}{M}\dot{\bar{\underset{\sim}{T}}}\underset{\sim}{M}^{T} = \underset{\sim}{M}\overline{\underset{\sim}{M}^{T}\underset{\sim}{T}\underset{\sim}{M}}^{\,\cdot}\underset{\sim}{M}^{T}. \tag{6}$$

The expressions of (6) show that the corotational rate of $\underset{\sim}{T}$ with respect to the reference frame $\underline{x}$ is obtained by finding the material rate of $\bar{\underset{\sim}{T}}$ with respect to frame $\bar{\underline{x}}$ and then transporting the result back to the reference frame $\underline{x}$.

It may be shown that the corotational rate is objective by considering a superposed rigid body rotation $\underset{\sim}{Q}$, such that $\underset{\sim}{M}' = \underset{\sim}{Q}\underset{\sim}{M}$ and $\underset{\sim}{T}' = \underset{\sim}{Q}\underset{\sim}{T}\underset{\sim}{Q}^{T}$. Therefore,

$$\overset{*}{\underset{\sim}{T}}{}' = \underset{\sim}{Q}\overset{*}{\underset{\sim}{T}}\underset{\sim}{Q}^{T}. \tag{7}$$

Let us now consider the integral $\Phi(\underset{\sim}{T})$ of the second order objective tensor $\underset{\sim}{T}$ [see Goddard and Miller (1966), Dafalias (1987)] which is a function of t and t', i.e. $\underset{\sim}{T} = \underset{\sim}{T}(t, t')$. In here t is the current time and t' is a dummy parameter of integration. Referring to the corotational frame $\bar{\underline{x}}$, the integral is defined as:

$$\Phi[\bar{\underset{\sim}{T}}] = \int_0^t \bar{\underset{\sim}{T}}(t, t')\,dt' = \int_0^t \underset{\sim}{M}^{T}(t')\underset{\sim}{T}(t, t')\underset{\sim}{M}(t')\,dt' = \underset{\sim}{M}^{T}(t)\Phi[\underset{\sim}{T}]\underset{\sim}{M}(t) \tag{8}$$

with

$$\Phi[\underset{\sim}{T}] = \underset{\sim}{M}(t)\left[\int_0^t \underset{\sim}{M}^{T}(t')\underset{\sim}{T}(t, t')\underset{\sim}{M}(t')\,dt'\right]\underset{\sim}{M}^{T}(t). \tag{9}$$

Physically, the corotational integral first transfers the tensor $\underset{\sim}{T}$ to the $\bar{\underline{x}}$ frame to obtain $\bar{\underset{\sim}{T}}$ and, after integration in the $\bar{\underline{x}}$ frame, it transports the result back to the $\underline{x}$ frame. Note that

$\underset{\sim}{T}(t')$ is a special case of $\underset{\sim}{T}(t, t')$. We now show that the corotational integral is objective by considering a superposed rigid body rotation $\underset{\sim}{Q}$, such that $\underset{\sim}{M}' = \underset{\sim}{Q}\underset{\sim}{M}$. In the eyes of the observer attached to the $\underline{x}'$ frame which has the rotation $\underset{\sim}{Q}$, the corotational integral is

$$\begin{aligned}\Phi'[\underset{\sim}{T}'] &= \underset{\sim}{M}'(t)\left[\int_0^t \underset{\sim}{M}'^{\mathrm{T}}(t')\underset{\sim}{T}'(t,t')\underset{\sim}{M}'(t')\,\mathrm{d}t'\right]\underset{\sim}{M}'^{\mathrm{T}}(t)\\ &= \underset{\sim}{Q}(t)\underset{\sim}{M}(t)\left[\int_0^t \underset{\sim}{M}^{\mathrm{T}}(t')\underset{\sim}{Q}^{\mathrm{T}}(t')\underset{\sim}{Q}(t')\underset{\sim}{T}(t,t')\underset{\sim}{Q}^{\mathrm{T}}(t')\underset{\sim}{Q}(t')\underset{\sim}{M}(t')\,\mathrm{d}t'\right]\underset{\sim}{M}^{\mathrm{T}}(t)\underset{\sim}{Q}^{\mathrm{T}}(t)\\ &= \underset{\sim}{Q}(t)\underset{\sim}{M}(t)\left[\int_0^t \underset{\sim}{M}^{\mathrm{T}}(t')\underset{\sim}{T}(t,t')\underset{\sim}{M}(t')\,\mathrm{d}t'\right]\underset{\sim}{M}^{\mathrm{T}}(t)\underset{\sim}{Q}^{\mathrm{T}}(t)\\ &= \underset{\sim}{Q}(t)\,\Phi[\underset{\sim}{T}]\underset{\sim}{Q}^{\mathrm{T}}(t).\end{aligned} \tag{10}$$

Equation (10) shows that the corotational integral $\Phi[\underset{\sim}{T}]$ is objective.

We can now find the relation between the corotational derivative and the corotational integral. We show that the corotational integration of the corotational derivative $\overset{*}{\underset{\sim}{T}}$ recovers the original tensor $\underset{\sim}{T}$, if $\underset{\sim}{T} = \underset{\sim}{T}(t')$, i.e. not a function of t. From (9), the corotational integral of $\overset{*}{\underset{\sim}{T}}$ is

$$\begin{aligned}\Phi[\overset{*}{\underset{\sim}{T}}] &= \underset{\sim}{M}(t)\left[\int_0^t \underset{\sim}{M}^{\mathrm{T}}(t')\overset{*}{\underset{\sim}{T}}(t')\underset{\sim}{M}(t')\,\mathrm{d}t'\right]\underset{\sim}{M}^{\mathrm{T}}(t) = \underset{\sim}{M}\int_0^t \dot{\bar{\underset{\sim}{T}}}(t')\,\mathrm{d}t'\,\underset{\sim}{M}^{\mathrm{T}}\\ &= \underset{\sim}{M}\bar{\underset{\sim}{T}}\underset{\sim}{M}^{\mathrm{T}} = \underset{\sim}{T}.\end{aligned} \tag{11}$$

The first equation of (6) was used in the above derivation. Equation (11) demonstrates that the corotational integral of a corotational rate of a tensor is the tensor itself. Therefore, the corotational integral is the inverse operation of the corotational derivative.

3. THE PLASTIC SPIN

The concept of plastic spin has been used frequently in the recent literature related to finite plastic deformation. It is the spin caused by plastic deformation. According to this concept, a portion of the total spin $\underset{\sim}{W}$ is absorbed by the plastic spin $\underset{\sim}{W}^{\mathrm{p}}$ and the rest is accommodated by a rigid body spin $\underset{\sim}{\omega}$ of the material macrostructure. Since we consider rigid–plastic deformation in this paper, we write

$$\underset{\sim}{\omega} = \underset{\sim}{W} - \underset{\sim}{W}^{\mathrm{p}} \tag{12}$$

and

$$\underset{\sim}{D} = \underset{\sim}{D}^{\mathrm{p}} \tag{13}$$

where $\underset{\sim}{D}$ is the rate of deformation tensor and is the symmetric part of the velocity gradient $\underset{\sim}{L}$, so that $\underset{\sim}{L} = \underset{\sim}{D} + \underset{\sim}{W}$. Equation (13) shows that the plastic part is the same as the total rate of deformation, and the elastic part has been neglected.

According to Dafalias (1985), the plastic spin $\underset{\sim}{W}^{\mathrm{p}}$ is a skew-symmetric isotropic function of $\underset{\sim}{\alpha}$ and $\underset{\sim}{\sigma}$, where $\underset{\sim}{\alpha}$ is the back stress tensor and $\underset{\sim}{\sigma}$ is the Cauchy stress tensor. The representation theorem of Wang (1970) for isotropic functions has then been used to obtain the following expression

$$\underset{\sim}{W}^{\mathrm{p}} = \eta_1(\underset{\sim}{\alpha}\underset{\sim}{\sigma}-\underset{\sim}{\sigma}\underset{\sim}{\alpha})+\eta_2(\underset{\sim}{\alpha}^2\underset{\sim}{\sigma}-\underset{\sim}{\sigma}\underset{\sim}{\alpha}^2)+\eta_3(\underset{\sim}{\alpha}\underset{\sim}{\sigma}^2-\underset{\sim}{\sigma}^2\underset{\sim}{\alpha})+\eta_4(\underset{\sim}{\alpha}\underset{\sim}{\sigma}\underset{\sim}{\alpha}^2-\underset{\sim}{\alpha}^2\underset{\sim}{\sigma}\underset{\sim}{\alpha})$$
$$+\eta_5(\underset{\sim}{\sigma}\underset{\sim}{\alpha}\underset{\sim}{\sigma}^2-\underset{\sim}{\sigma}^2\underset{\sim}{\alpha}\underset{\sim}{\sigma}) \quad (14)$$

where η_i's are scalar functions of the isotropic invariants of $\underset{\sim}{\sigma}$ and $\underset{\sim}{\alpha}$.

Since the rigid body spin of the material macrostructure is $\underset{\sim}{\omega}$, we write the corotational rate of the back stress as

$$\overset{*}{\underset{\sim}{\alpha}} = \dot{\underset{\sim}{\alpha}}-\underset{\sim}{\omega}\underset{\sim}{\alpha}+\underset{\sim}{\alpha}\underset{\sim}{\omega}. \quad (15)$$

4. THE ENDOCHRONIC THEORY

According to the endochronic theory of Valanis (1980) by assuming that the material is plastically incompressible, we have the following constitutive equation for small deformation

$$\underset{\sim}{s} = S_y\frac{\mathrm{d}\underset{\sim}{\varepsilon}^{\mathrm{p}}}{\mathrm{d}z}+\int_0^z \mu(z-z')\frac{\mathrm{d}\underset{\sim}{\varepsilon}^{\mathrm{p}}}{\mathrm{d}z'}\,\mathrm{d}z'. \quad (16)$$

In the above equation $\underset{\sim}{s}$ is the deviatoric stress; $\underset{\sim}{\varepsilon}$ is the strain; $\underset{\sim}{\varepsilon}^{\mathrm{p}} = \underset{\sim}{\varepsilon}-\underset{\sim}{s}/G$ is the plastic strain; G is the shear modulus; $S_y = \sqrt{2}\,\tau_y$ where τ_y is the initial yield stress in shear; $\mu(z)$ is the kernel function; and z is the intrinsic time which is used to register histories of plastic deformation. Equation (16) may be rewritten as

$$\underset{\sim}{s}-\underset{\sim}{\alpha} = S_y\frac{\mathrm{d}\underset{\sim}{\varepsilon}^{\mathrm{p}}}{\mathrm{d}z} = S_y f(z)\frac{\mathrm{d}\underset{\sim}{\varepsilon}^{\mathrm{p}}}{\mathrm{d}\zeta} \quad (17)$$

where

$$f(z) = \frac{\mathrm{d}\zeta}{\mathrm{d}z} = c-(c-1)\,\mathrm{e}^{-\beta z} \quad (18)$$

$$\mathrm{d}\zeta^2 = \mathrm{d}\underset{\sim}{\varepsilon}^{\mathrm{p}}\cdot\mathrm{d}\underset{\sim}{\varepsilon}^{\mathrm{p}} \quad (19)$$

and

$$\underset{\sim}{\alpha} = \int_0^z \mu(z-z')\frac{\mathrm{d}\underset{\sim}{\varepsilon}^{\mathrm{p}}}{\mathrm{d}z'}\,\mathrm{d}z'. \quad (20)$$

The intrinsic time z is scaled by a function $f(z)$, so that another intrinsic time ζ is defined through (18). The intrinsic time ζ is further defined in terms of the plastic strain by eqn (19) so that ζ accumulates monotonically whenever plastic deformation occurs. The function $f(z)$ has been shown to represent isotropic strain hardening and is referred to as the isotropic hardening function. Parameter c specifies the saturated state and β the rate of approaching the saturated state of isotropic hardening. The back stress $\underset{\sim}{\alpha}$, given by the integral in eqn (20), specifies the position of the center of yield surface.

By using eqn (17), eqn (19) leads to

$$\left[\left(\frac{\underset{\sim}{s}-\underset{\sim}{\alpha}}{S_y f}\right)\cdot\left(\frac{\underset{\sim}{s}-\underset{\sim}{\alpha}}{S_y f}\right)-1\right]\mathrm{d}\zeta^2 = 0. \quad (21)$$

Thus, either

$$\mathrm{d}\zeta \neq 0 \quad \text{and} \quad \left(\frac{\underset{\sim}{s}-\underset{\sim}{\alpha}}{S_y f}\right)\cdot\left(\frac{\underset{\sim}{s}-\underset{\sim}{\alpha}}{S_y f}\right)-1 = 0 \tag{22}$$

or

$$\mathrm{d}\zeta = 0 \quad \text{and} \quad \left(\frac{\underset{\sim}{s}-\underset{\sim}{\alpha}}{S_y f}\right)\cdot\left(\frac{\underset{\sim}{s}-\underset{\sim}{\alpha}}{S_y f}\right)-1 \neq 0. \tag{23}$$

Equation (22) represents plastic deformation obeying the Mises yield criterion with combined isotropic–kinematic hardening, while eqn (23) represents the elastic state governed by Hooke's law $\mathrm{d}\underset{\sim}{s} = G\,\mathrm{d}\underset{\sim}{\varepsilon}$. Since the elastic state is inside of the yield surface, the second expression in (23) is justified. Equation (22) is further written as

$$(\underset{\sim}{s}-\underset{\sim}{\alpha})\cdot(\underset{\sim}{s}-\underset{\sim}{\alpha}) = S_y^2 f(z)^2 \tag{24}$$

in which the meanings of $f(z)$ and $\underset{\sim}{\alpha}$ are readily visualized.

On the other hand, the expression for the plastic strain increment is

$$\mathrm{d}\underset{\sim}{\varepsilon}^{\mathrm{p}} = \frac{1}{S_y}(\underset{\sim}{s}-\underset{\sim}{\alpha})\,\mathrm{d}z \tag{25}$$

which is obtained from eqn (17) and may be regarded as the flow rule.

We see that starting with the integral form of eqn (16), the endochronic constitutive equation is now written in the incremental form given by eqn (25), with the yield function governed by eqn (24). Mathematically speaking, the integral and incremental forms are equivalent provided that appropriate initial conditions are used.

We now extend the above model to the finite deformation range. To this end, eqns (18) and (25) are written as:

$$\zeta^2 = \underset{\sim}{D}\cdot\underset{\sim}{D} \tag{26}$$

$$\underset{\sim}{D} = \frac{1}{S_y}(\underset{\sim}{s}-\underset{\sim}{\alpha})\dot{z}. \tag{27}$$

Note that the constitutive eqn (27) is in incremental form; only the back stress $\underset{\sim}{\alpha}$ given by (20) is in integral form. We extend expression (20) to the case of large deformation by use of (9) and consider a second order tensor $\mu(z,z')(\underset{\sim}{D}/\dot{z}')$. In this expression, $\dot{z} \neq 0$, since the case of $\dot{z} = 0$ corresponds to the elastic behavior. Then $\underset{\sim}{\alpha}$ is the corotational integral $\Phi[\mu(z,z')(\underset{\sim}{D}/\dot{z}')]$ in the case of large deformation. It follows that

$$\underset{\sim}{\alpha} = \underset{\sim}{M}(z)\left[\int_0^z \mu(z-z')\frac{\underset{\sim}{M}^{\mathrm{T}}(z')\underset{\sim}{D}\underset{\sim}{M}(z')}{\dot{z}'}\,\mathrm{d}z'\right]\underset{\sim}{M}^{\mathrm{T}}(z). \tag{28}$$

The integration in (28) is with respect to z' which is not t' as in (9). The intrinsic time z is a monotonically increasing parameter and it does not change during elastic deformation or rigid body rotation. In general, $\underset{\sim}{M}(z)$ is not a unique function of z, because rotation may continue even when z is not changing. This multivalued association of $\underset{\sim}{M}(z)$ to z does not invalidate the meaning of integral (28) as pointed out by Dafalias (1987).

For simplicity in the subsequent calculations, we consider

$$\mu(z) = \mu_1 \exp(-\lambda_1 z)+\mu_2$$

with

$$\mu(0) = \mu_1 + \mu_2. \tag{29}$$

Then, eqn (28) becomes

$$\underset{\sim}{\alpha} = \underset{\sim}{\alpha}^{(1)} + \underset{\sim}{\alpha}^{(2)} \tag{30}$$

where

$$\underset{\sim}{\alpha}^{(1)} = \mu_1 \underset{\sim}{M}(z) \left[\int_0^z e^{-\lambda_1(z-z')} \frac{\underset{\sim}{M}^T(z')\underset{\sim}{D}\underset{\sim}{M}(z')}{\dot{z}'} \, dz' \right] \underset{\sim}{M}^T(z) \tag{31}$$

and

$$\underset{\sim}{\alpha}^{(2)} = \mu_2 \underset{\sim}{M}(z) \left[\int_0^z \frac{\underset{\sim}{M}^T(z')\underset{\sim}{D}\underset{\sim}{M}(z')}{\dot{z}'} \, dz' \right] \underset{\sim}{M}^T(z). \tag{32}$$

Since $\underset{\sim}{\alpha}$ is a tensor, we have from (2)

$$\bar{\underset{\sim}{\alpha}} = \underset{\sim}{M}^T \underset{\sim}{\alpha} \underset{\sim}{M}. \tag{33}$$

We then have the corotational rate of $\underset{\sim}{\alpha}$ given by (6) as

$$\overset{*}{\underset{\sim}{\alpha}} = \underset{\sim}{M} \dot{\bar{\underset{\sim}{\alpha}}} \underset{\sim}{M}^T = \underset{\sim}{M} \frac{d\bar{\underset{\sim}{\alpha}}}{dz} \dot{z} \underset{\sim}{M}^T. \tag{34}$$

By use of (28) and differentiating the expression for $\bar{\underset{\sim}{\alpha}} = \underset{\sim}{M}^T \underset{\sim}{\alpha} \underset{\sim}{M}$ and then substituting the resulting expression into eqn (34), we find

$$\begin{aligned} \overset{*}{\underset{\sim}{\alpha}} &= \dot{z} \left[\mu(0) \frac{\underset{\sim}{D}}{\dot{z}} - \lambda_1 \underset{\sim}{\alpha}^{(1)} \right] \\ &= (\mu_1 + \mu_2)\underset{\sim}{D} - \lambda_1 \underset{\sim}{\alpha} \dot{z} + \lambda_1 \underset{\sim}{\alpha}^{(2)} \dot{z}. \end{aligned} \tag{35}$$

Equation (35) is the evolution equation of the back stress in terms of the plastic strain rate $\underset{\sim}{D}$, the back stress $\underset{\sim}{\alpha}$ and the intrinsic time z. Note that eqn (35) is in incremental form, except for $\underset{\sim}{\alpha}^{(2)}$ which is represented by an integral in eqn (32). It will be shown in the next section that in solving the problem of thin-walled tubes under torsion, this integral may be integrated so that eqn (35) becomes a true incremental form.

By using a similar procedure as in eqn (14) and retaining only the first term for simplicity, the plastic spin for this theory is written as

$$\underset{\sim}{W}^p = \frac{C_1 \dot{\zeta}}{S_y^2 f(z)^2} (\underset{\sim}{\alpha}\underset{\sim}{s} - \underset{\sim}{s}\underset{\sim}{\alpha}) \tag{36}$$

where C_1 is dimensionless and is a scalar function of the isotropic invariants of $\underset{\sim}{s}$ and $\underset{\sim}{\alpha}$; $\dot{\zeta}$ is the rate of intrinsic time; and $f(z)$ is given by eqn (18). Using the first expression of eqn (18), eqn (36) becomes:

$$\begin{aligned} \underset{\sim}{W}^p &= \frac{C_1 f(z) \dot{z}}{S_y^2 f(z)^2} (\underset{\sim}{\alpha}\underset{\sim}{s} - \underset{\sim}{\alpha}^2 + \underset{\sim}{\alpha}^2 - \underset{\sim}{s}\underset{\sim}{\alpha}) \\ &= \frac{C_1}{S_y f(z)} \left[\underset{\sim}{\alpha} \frac{(\underset{\sim}{s} - \underset{\sim}{\alpha})\dot{z}}{S_y} + \frac{(\underset{\sim}{\alpha} - \underset{\sim}{s})\dot{z}}{S_y} \underset{\sim}{\alpha} \right] \end{aligned}$$

$$= \frac{C_1}{S_y f(z)}(\underset{\sim}{\alpha}\underset{\sim}{D} - \underset{\sim}{D}\underset{\sim}{\alpha}) = K(\underset{\sim}{\alpha}\underset{\sim}{D} - \underset{\sim}{D}\underset{\sim}{\alpha}). \tag{37}$$

Equation (25) is used in the last two expressions, and the coefficient K is given by

$$K = \frac{C_1}{S_y f(z)}. \tag{38}$$

The above expressions are consistent with the results of Dafalias (1985) using a different theory. Equation (37) together with eqn (12) are substituted into eqn (35) when the corotational rate is used in the calculation.

5. THIN-WALLED TUBE UNDER TORSION

In the consideration of thin-walled tubes under torsion in the large strain range, the elastic strain is neglected, so that the condition of plastic incompressibility is represented by

$$\dot{\varepsilon}_r + \dot{\varepsilon}_\theta + \dot{\varepsilon}_z = 0 \tag{39}$$

where $\dot{\varepsilon}_r$ denotes the strain rate in the radial direction; $\dot{\varepsilon}_\theta$ denotes the strain rate in the tangential direction; and $\dot{\varepsilon}_z$ denotes the strain rate in the axial direction of the tube. The shear strain 2η is related to the angle of twist per unit length φ by

$$2\eta = \mathrm{r}\varphi \tag{40}$$

in which r is the outer radius of the tube. The rate of deformation and spin tensors are expressed as

$$\underset{\sim}{D} = \begin{bmatrix} \dot{\varepsilon}_r & 0 & 0 \\ 0 & \dot{\varepsilon}_\theta & \dot{\eta} \\ 0 & \dot{\eta} & \dot{\varepsilon}_z \end{bmatrix} \tag{41}$$

and

$$\underset{\sim}{W} = \begin{bmatrix} 0 & 0 & 0 \\ 0 & 0 & \dot{\eta} \\ 0 & -\dot{\eta} & 0 \end{bmatrix}. \tag{42}$$

Equations (41) and (42) are now used to derive the explicit expressions for plastic spin and back stress.

Let the back stress be symmetric so that

$$\underset{\sim}{\alpha} = \begin{bmatrix} \alpha_{rr} & 0 & 0 \\ 0 & \alpha_{\theta\theta} & \alpha_{\theta z} \\ 0 & \alpha_{\theta z} & \alpha_{zz} \end{bmatrix}. \tag{43}$$

Then, since $\underset{\sim}{D}$ and $\underset{\sim}{\alpha}$ are symmetric, we note that $\underset{\sim}{D}\underset{\sim}{\alpha} = (\underset{\sim}{\alpha}\underset{\sim}{D})^T$. Therefore,

$$\underset{\sim}{\alpha}\underset{\sim}{D}-\underset{\sim}{D}\underset{\sim}{\alpha}=\begin{bmatrix}0 & 0 & 0\\ 0 & 0 & (\alpha_{\theta\theta}-\alpha_{zz})\dot{\eta}+\alpha_{\theta z}(\dot{\varepsilon}_z-\dot{\varepsilon}_\theta)\\ 0 & -(\alpha_{\theta\theta}-\alpha_{zz})\dot{\eta}-\alpha_{\theta z}(\dot{\varepsilon}_z-\dot{\varepsilon}_\theta) & 0\end{bmatrix}. \quad (44)$$

Equation (44) is substituted in eqn (37) to calculate the plastic spin $\underset{\sim}{W}^p$. On the other hand, the rigid body spin $\underset{\sim}{\omega}$ is defined in eqn (12) as:

$$\underset{\sim}{\omega}=\underset{\sim}{W}-\underset{\sim}{W}^p=\begin{bmatrix}0 & 0 & 0\\ 0 & 0 & -\omega\\ 0 & \omega & 0\end{bmatrix} \quad (45)$$

where

$$\omega = K[(\alpha_{\theta\theta}-\alpha_{zz})\dot{\eta}+\alpha_{\theta z}(\dot{\varepsilon}_z-\dot{\varepsilon}_\theta)]-\dot{\eta}. \quad (46)$$

Since the tensor $\underset{\sim}{\alpha}$ is symmetric and the tensor $\underset{\sim}{\omega}$ is antisymmetric, we have $\underset{\sim}{\alpha}\underset{\sim}{\omega} = -(\underset{\sim}{\omega}\underset{\sim}{\alpha})^T$. Therefore, in order to find explicit expressions for the corotational rate, we first find

$$\underset{\sim}{\omega}\underset{\sim}{\alpha}-\underset{\sim}{\alpha}\underset{\sim}{\omega}=\begin{bmatrix}0 & 0 & 0\\ 0 & -2\omega\alpha_{\theta z} & -\omega(\alpha_{zz}-\alpha_{\theta\theta})\\ 0 & -\omega(\alpha_{zz}-\alpha_{\theta\theta}) & 2\omega\alpha_{\theta z}\end{bmatrix} \quad (47)$$

and then obtain the following expressions by combining (15) and (35)

$$\begin{aligned}\dot{\underset{\sim}{\alpha}} &= \underset{\sim}{\omega}\underset{\sim}{\alpha}-\underset{\sim}{\alpha}\underset{\sim}{\omega}+\overset{*}{\underset{\sim}{\alpha}}\\ &= (\underset{\sim}{\omega}\underset{\sim}{\alpha}-\underset{\sim}{\alpha}\underset{\sim}{\omega})+(\mu_1+\mu_2)\underset{\sim}{D}-\lambda_1\underset{\sim}{\alpha}\dot{z}+\lambda_1\underset{\sim}{\alpha}^{(2)}\dot{z}\end{aligned} \quad (48)$$

where, from (32),

$$\underset{\sim}{\alpha}^{(2)} = \mu_2\int_0^z \frac{\underset{\sim}{D}}{\dot{z}'}\,dz'. \quad (49)$$

In the last expression, it has been assumed that the corotational axes are parallel to the reference axes, so that $\underset{\sim}{M}=\underset{\sim}{I}$. This is indeed the case for the torsion problems under consideration. The deformation is homogeneous and the angle of twist per unit length is constant along the tube.

In the numerical calculation, we can define a tensor $\underset{\sim}{\Phi}$ as

$$\underset{\sim}{\Phi}=\underset{\sim}{\omega}\,dt=\begin{bmatrix}0 & 0 & 0\\ 0 & 0 & -\Phi\\ 0 & \Phi & 0\end{bmatrix} \quad (50)$$

in which the following expression has been determined by use of eqn (46)

$$\Phi = \omega dt = K[(\alpha_{\theta\theta}-\alpha_{zz})d\eta+\alpha_{\theta z}(d\varepsilon_z-d\varepsilon_\theta)]-d\eta \quad (51)$$

Then, (48) reduces to

$$d\underset{\sim}{\alpha} = (\Phi\underset{\sim}{\alpha} - \underset{\sim}{\alpha}\Phi) + (\mu_1 + \mu_2)\underset{\sim}{D}\, dt - \lambda_1 \underset{\sim}{\alpha}\, dz + \lambda_1 \underset{\sim}{\alpha}^{(2)}\, dz. \tag{52}$$

The equations derived in this section can be used to describe the response of a thin-walled tube subjected to various combined axial–torsional loading conditions. Two special cases are considered in the following.

(A) *Torsion with axial prestress*

Denoting the axial prestress by $\sigma_z = \sigma_c$ = constant, the stress tensor and the deviatoric stress tensor are

$$\underset{\sim}{\sigma} = \begin{bmatrix} 0 & 0 & 0 \\ 0 & 0 & \tau \\ 0 & \tau & \sigma_c \end{bmatrix} \quad \text{and} \quad \underset{\sim}{s} = \begin{bmatrix} \frac{-\sigma_c}{3} & 0 & 0 \\ 0 & \frac{-\sigma_c}{3} & \tau \\ 0 & \tau & \frac{2\sigma_c}{3} \end{bmatrix}. \tag{53}$$

Note that the hoop stress σ_θ is zero due to symmetry. The constitutive equations are, from eqns (27), (41), (43) and (53), written as

$$\begin{aligned} \frac{d\varepsilon_r}{dz} &= -\frac{\frac{\sigma_c}{3} + \alpha_{rr}}{S_y} \\ \frac{d\varepsilon_\theta}{dz} &= -\frac{\frac{\sigma_c}{3} + \alpha_{\theta\theta}}{S_y} \\ \frac{d\varepsilon_z}{dz} &= \frac{\frac{2\sigma_c}{3} - \alpha_{zz}}{S_y} \\ \frac{d\eta}{dz} &= \frac{\tau - \alpha_{\theta z}}{S_y}. \end{aligned} \tag{54}$$

The intrinsic time is then given from eqns (26) and (41) by

$$\dot{\zeta}^2 = \dot{\varepsilon}_r^2 + \dot{\varepsilon}_\theta^2 + \dot{\varepsilon}_z^2 + 2\dot{\eta}^2 = \dot{z}^2 f^2(z). \tag{55}$$

Therefore,

$$\dot{\eta}^2 = \tfrac{1}{2}[\dot{z}^2 f^2(z) - (\dot{\varepsilon}_r^2 + \dot{\varepsilon}_\theta^2 + \dot{\varepsilon}_z^2)]. \tag{56}$$

By use of eqn (39), eqn (56) reduces to

$$\begin{aligned} \dot{\eta}^2 &= \tfrac{1}{2}[\dot{z}^2 f^2(z) - 2(\dot{\varepsilon}_z^2 - \dot{\varepsilon}_\theta \dot{\varepsilon}_r)] \\ &= \tfrac{1}{2}\dot{z}^2\left[f^2(z) - 2\left(\left(\frac{d\varepsilon_z}{dz}\right)^2 - \left(\frac{d\varepsilon_\theta}{dz}\right)\left(\frac{d\varepsilon_r}{dz}\right)\right)\right]. \end{aligned} \tag{57}$$

Substituting eqn (54) in eqn (57), we then obtain

$$\pm \mathrm{d}\eta = \mathrm{d}z \sqrt{\tfrac{1}{2} f^2(z) - \left(\frac{1}{S_y}\right)^2 \left(\left(\frac{2\sigma_c}{3} - \alpha_{zz}\right)^2 - \left(\frac{\sigma_c}{3} + \alpha_{rr}\right)\left(\frac{\sigma_c}{3} + \alpha_{\theta\theta}\right)\right)}. \tag{58}$$

The "+" sign is for loading and "−" is for unloading.

To perform the numerical calculation of $\mathrm{d}\underset{\sim}{\alpha}$ by use of eqn (52), $\underset{\sim}{\alpha}^{(2)}$ must first be determined. To obtain $\alpha_{\theta z}^{(2)}$ from eqn (49), we use eqn (41) to get

$$\alpha_{\theta z}^{(2)} = \mu_2 \int_0^z \frac{D_{\theta z}}{\dot{z}'}\,\mathrm{d}z' = \mu_2 \int_{\eta(0)}^{\eta(z)} \mathrm{d}\eta = \mu_2 \eta. \tag{59}$$

In the last expression, the limits of integration are $\eta(0) = 0$ and $\eta(z) = \eta$. Similarly, we obtain the following components for $\underset{\sim}{\alpha}^{(2)}$ during loading:

$$\begin{aligned} \alpha_{rr}^{(2)} &= \mu_2 \varepsilon_r \\ \alpha_{\theta\theta}^{(2)} &= \mu_2 \varepsilon_\theta \\ \alpha_{zz}^{(2)} &= \mu_2 \varepsilon_z \end{aligned} \tag{60}$$

Therefore, from eqns (50), (52), (59) and (60), we obtain the following equations:

$$\begin{aligned} \mathrm{d}\alpha_{rr} &= (\mu_1 + \mu_2)\,\mathrm{d}\varepsilon_r - \lambda_1 \alpha_{rr}\,\mathrm{d}z + \lambda_1 \mu_2 \varepsilon_r\,\mathrm{d}z \\ \mathrm{d}\alpha_{\theta\theta} &= -2\alpha_{\theta z}\Phi + (\mu_1 + \mu_2)\,\mathrm{d}\varepsilon_\theta - \lambda_1 \alpha_{\theta\theta}\,\mathrm{d}z + \lambda_1 \mu_2 \varepsilon_\theta\,\mathrm{d}z \\ \mathrm{d}\alpha_{zz} &= 2\alpha_{\theta z}\Phi + (\mu_1 + \mu_2)\,\mathrm{d}\varepsilon_z - \lambda_1 \alpha_{zz}\,\mathrm{d}z + \lambda_1 \mu_2 \varepsilon_z\,\mathrm{d}z \\ \mathrm{d}\alpha_{\theta z} &= (\alpha_{\theta\theta} - \alpha_{zz})\Phi + (\mu_1 + \mu_2)\,\mathrm{d}\eta - \lambda_1 \alpha_{\theta z}\,\mathrm{d}z + \lambda_1 \mu_2 \eta\,\mathrm{d}z \end{aligned} \tag{61}$$

with the initial conditions $\eta(0) = 0$, $\varepsilon_i(0) = 0$, and $\alpha_{ij}(0) = 0$. Thus, in a step by step calculation, we can use

$$\begin{aligned} \underset{\sim}{\alpha} &= \underset{\sim}{\alpha} + \mathrm{d}\underset{\sim}{\alpha} \\ \varepsilon_r &= \varepsilon_r + \mathrm{d}\varepsilon_r \\ \varepsilon_\theta &= \varepsilon_\theta + \mathrm{d}\varepsilon_\theta \\ \varepsilon_z &= \varepsilon_z + \mathrm{d}\varepsilon_z \\ \eta &= \eta + \mathrm{d}\eta. \end{aligned} \tag{62}$$

Finally, we note that for the case of pure torsion, the ends of the specimen are totally unconstrained with $\sigma_c = 0$. Thus, the equations for pure torsion may be obtained by setting $\sigma_c = 0$ in the equations of this subsection.

(B) *Simple torsion*

In the case of simple torsion, the ends of the tube are fixed so that $\dot{\varepsilon}_z = 0$. Assuming incompressibility, we find from (39) that $\dot{\varepsilon}_\theta = -\dot{\varepsilon}_r \neq 0$. Hence, (41) becomes

$$\underset{\sim}{D} = \begin{bmatrix} \dot{\varepsilon}_r & 0 & 0 \\ 0 & -\dot{\varepsilon}_r & \dot{\eta} \\ 0 & \dot{\eta} & 0 \end{bmatrix}. \tag{63}$$

Note that this is different from the simple shear assumption where $\dot{\varepsilon}_\theta = 0$. The stress tensor and the deviatoric stress tensor are

$$\underset{\sim}{\sigma} = \begin{bmatrix} 0 & 0 & 0 \\ 0 & 0 & \tau \\ 0 & \tau & \sigma \end{bmatrix} \quad \text{and} \quad \underset{\sim}{s} = \begin{bmatrix} \frac{-\sigma}{3} & 0 & 0 \\ 0 & \frac{-\sigma}{3} & \tau \\ 0 & \tau & \frac{2\sigma}{3} \end{bmatrix} \tag{64}$$

in which $\underset{\sim}{\sigma}$ may vary. Again, we mention that the hoop stress is zero which is different from the simple shear assumption that $\sigma_\theta \neq 0$. The constitutive equation, from eqn (27), has the following component equations:

$$\begin{aligned} \alpha_{rr} + S_y \frac{d\varepsilon_r}{dz} &= \frac{-\sigma}{3} \\ \alpha_{\theta\theta} - S_y \frac{d\varepsilon_r}{dz} &= \frac{-\sigma}{3} \\ \alpha_{zz} &= \frac{2\sigma}{3} \\ \alpha_{\theta z} + S_y \frac{d\eta}{dz} &= \tau. \end{aligned} \tag{65}$$

The first two equations of (65) may be combined to yield

$$\frac{d\varepsilon_r}{dz} = \frac{\alpha_{\theta\theta} - \alpha_{rr}}{2S_y}. \tag{66}$$

The intrinsic time is then, from eqn (26) and eqn (63), given by

$$\dot{\zeta}^2 = 2\dot{\varepsilon}_r^2 + 2\dot{\eta}^2 = \dot{z}^2 f^2(z). \tag{67}$$

Therefore,

$$\dot{\eta}^2 = \dot{z}^2 \left[\frac{1}{2} f^2(z) - \left(\frac{d\varepsilon_r}{dz} \right)^2 \right]. \tag{68}$$

Then, by substituting (66) in (68), we obtain

$$\pm d\eta = dz \sqrt{\frac{f^2(z)}{2} - \left(\frac{\alpha_{\theta\theta} - \alpha_{rr}}{2S_y} \right)^2}. \tag{69}$$

The "+" sign is for loading and "−" is for unloading.

We may also obtain the following components of $\underset{\sim}{\alpha}^{(2)}$ by using the same procedure as that leads to eqns (59) and (60)

$$\begin{aligned} \alpha_{\theta z}^{(2)} &= \mu_2 \eta \\ \alpha_{rr}^{(2)} &= \mu_2 \varepsilon_r \\ \alpha_{\theta\theta}^{(2)} &= -\mu_2 \varepsilon_r \\ \alpha_{zz}^{(2)} &= 0. \end{aligned} \tag{70}$$

Therefore, from (50–52) and (70), we obtain the following component equations

$$
\begin{aligned}
d\alpha_{rr} &= (\mu_1+\mu_2)\,d\varepsilon_r - \lambda_1\alpha_{rr}\,dz + \lambda_1\mu_2\varepsilon_r\,dz \\
d\alpha_{\theta\theta} &= -2\alpha_{\theta z}\Phi - (\mu_1+\mu_2)\,d\varepsilon_r - \lambda_1\alpha_{\theta\theta}\,dz - \lambda_1\mu_2\,\varepsilon_r\,dz \\
d\alpha_{zz} &= 2\alpha_{\theta z}\Phi - \lambda_1\alpha_{zz}\,dz \\
d\alpha_{\theta z} &= (\alpha_{\theta\theta}-\alpha_{zz})\Phi + (\mu_1+\mu_2)\,d\eta - \lambda_1\alpha_{\theta z}\,dz + \lambda_1\mu_2\eta\,dz
\end{aligned} \tag{71}
$$

with the initial conditions $\eta(0) = 0$, $\varepsilon_r(0) = 0$, and $\alpha_{ij}(0) = 0$. We again use eqn (62) for a step by step calculation.

6. COMPARISON OF THEORETICAL AND EXPERIMENTAL RESULTS

In this section, we compare the theoretical and experimental results. There are seven material constants in our model: c, β, C_1, S_y, μ_1, μ_2 and λ_1 where c and β are used in the hardening function $f(z)$ and describe the rate and saturation value of isotropic hardening; C_1 fixes the magnitude of plastic spin; S_y is a material constant proportional to the initial yield stress in shear ($S_y = \sqrt{2}\tau_y$); and μ_1, μ_2 and λ_1 are used in the kernel function $\mu(z)$ which describes the evolution of back stress. These material constants are determined by fitting the theory to the experimental stress–strain curve during loading. After they have been determined, the constitutive equations are applied to predict experimental results of specimens subjected to different loading conditions. Three different materials have been investigated, 70 : 30 brass, Ni-200 and Al-1100. All shear strains reported in the experimental results are for the outer surface of the tubular specimen.

For the 70 : 30 brass material, the material constants have been determined to fit the experimental data of Stout [reported in Im and Atluri (1987)] for the case of simple torsion, Fig. 1. The constants are: $c = 3.1$, $\beta = 15.4$, $C_1 = 4.5$, $S_y = 90$ MPa, $\mu_1 = 200$ MPa, $\mu_2 = 50$ MPa and $\lambda_1 = 7.2$. These constants are then used in the equations for torsion with axial stress $\sigma_c = 0$ [equations in Section 5(A)] to predict behavior of the same material for two different strain paths, i.e. monotonic and cyclic pure torsion. The strain range of the monotonic pure torsion is from 0 to 4, whereas the specimen under cyclic pure torsional loading is strained from 0 to 1.7, unstrained back to 0, and then, restrained to 2.0. The

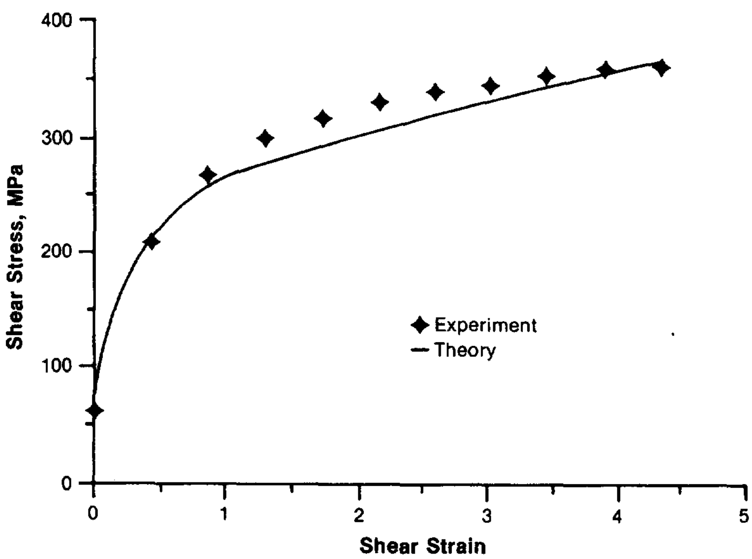

Fig. 1. Shear stress–strain curve of 70 : 30 brass.

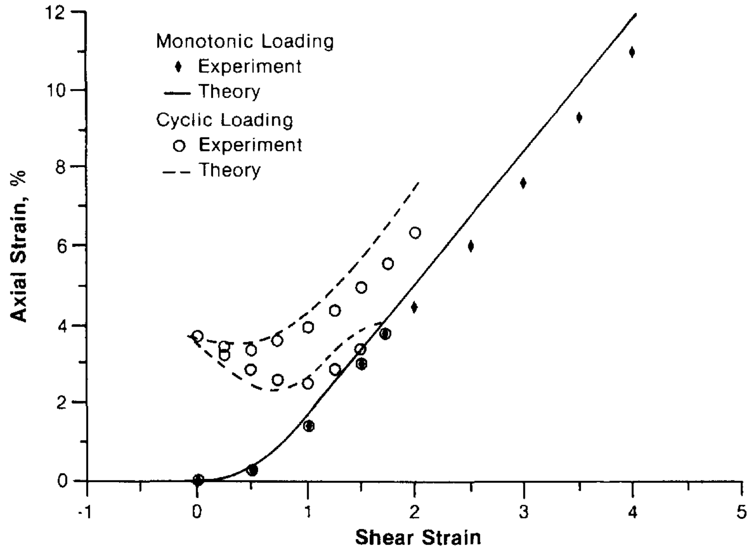

Fig. 2. Monotonic and cyclic axial–shear strain curves of 70 : 30 brass.

results found from this theory are compared with the experimental data of Swift (1947). Figure 2 shows results of both monotonic and cyclic pure torsion. It is seen that the theory does predict the trend of variation for the axial strain during torsion. We note that experiments of Swift and Stout were conducted in different laboratories and material conditions, and the agreement demonstrated here is therefore considered as very satisfactory. The effect of C_1 is investigated and shown in Fig. 3 for 70 : 30 brass. This figure shows the dependence of the axial strain on C_1 in the case of monotonic pure torsion. It is seen that a suitable C_1 can be determined to achieve a good agreement with the experimental results.

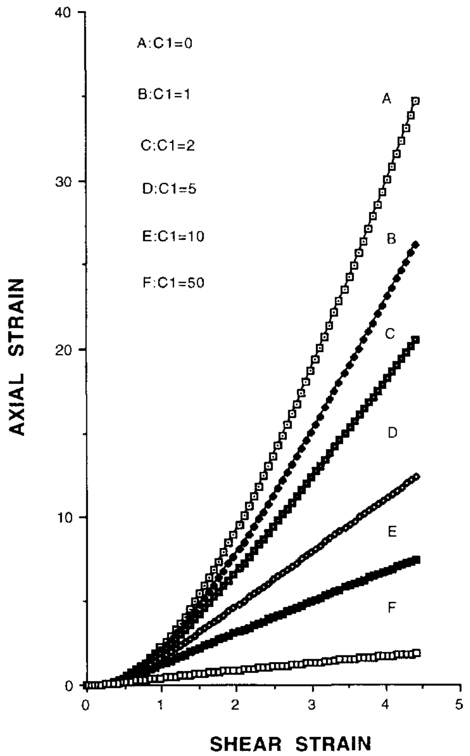

Fig. 3. Effect of plastic spin on the axial strain for 70 : 30 brass during pure torsion.

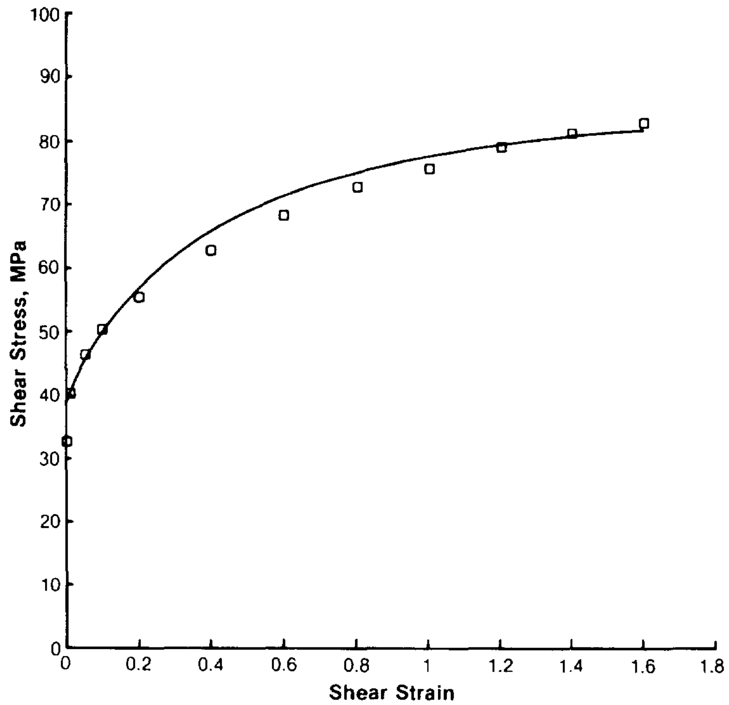

Fig. 4. Shear stress–strain curve of Ni-200 at prestress = 0.01 MPa.

The experimental data for Ni-200 are taken from Hart and Chang (1985). The material constants have been determined by fitting the shear stress–strain curve (Fig. 4) which was determined from torsion with a 0.01 MPa prestress. The constants have been determined to be: $c = 14.2$, $\beta = 5.5$, $C_1 = 9$, $S_y = 40$ MPa, $\mu_1 = 45$ MPa, $\mu_2 = 40$ MPa and $\lambda_1 = 9.5$. Using these constants and constitutive equations of Section 5(A), we have predicted the axial strain associated with torsion with prestresses of 1.48, 0.01 and -1.52 MPa. The results, shown in Fig. 5, are quite satisfactory.

Figure 6 shows the experimental shear stress–strain curve under simple shear conditions, obtained by White *et al.* (1990), for Al-1100 material. The theoretical result of the present theory is also shown. The material constants are $c = 2.14$, $\beta = 4.5$, $C_1 = 4.5$, $S_y = 55$ MPa, $\mu_1 = 1.8$ MPa, $\mu_2 = 0.15$ MPa and $\lambda_1 = 1.64$. Wu and Xu (1989) also obtained a shear stress–strain curve of Al-1100, but in a smaller deformation range (12% strain). The curve agrees with the one shown in Fig. 6. Using these constants and constitutive equations of Section 5(A), we predicted the axial strain in the case of torsion with prestresses of -6.9 and -20.7 MPa. The results found from this theory are (the solid and dashed curves) compared with the experimental data of Wu and Xu (1989) and shown in Fig. 7. Figure 8 shows the prediction (the solid and dashed curves) of the hoop and axial strains, respectively, for the pure torsion condition (i.e. with $\sigma_c = 0$). The experimental data of Bailey *et al.* (1972) are also shown in the figure. Even though the theory agrees well with experiment in the axial strain, there are discrepancies in the hoop strain at large shear strain level. These discrepancies may be explained by taking a closer look at the specimens and the procedure used in the experiments of Bailey *et al.* (1972). The specimens used by them had a very short gauge length of 0.125″ compared to a radius of 0.75″. The radius of the relatively rigid ends of the specimen did not change, which in turn restricted the development of hoop strain at large shear strain level. Another possible restriction to the hoop strain is due to a plug and sleeve inserted by the authors to prevent buckling at large strain levels. The authors thought that there was sufficient clearance to allow for any reduction in diameter during testing. However, we believe that there was contact between the specimens and the plug at large shear strain levels and, therefore, the reduction in diameter was restricted. If there were no contact, then the plug would not have been needed in the experiment. We believe that these are the reasons causing the experimental hoop strain to

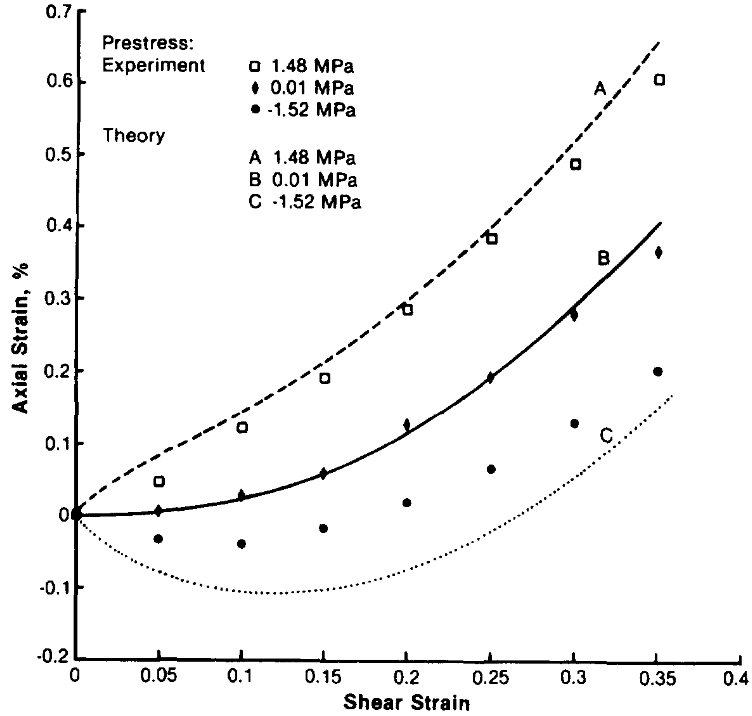

Fig. 5. Axial–shear strain curves with various axial prestresses (Ni-200).

be on the low side compared to the theoretical result. Wu *et al.* (1994b) conducted the same experiments by use of extruded high purity aluminum with specimens of a much longer gauge length (3.25″) and without the plug. The outer radius of the specimens was 0.75″. The results are shown in Fig. 9. It is seen that these curves have the same trends as those of the theoretical curves shown in Fig. 8, i.e. the hoop and axial strains at large shear strain

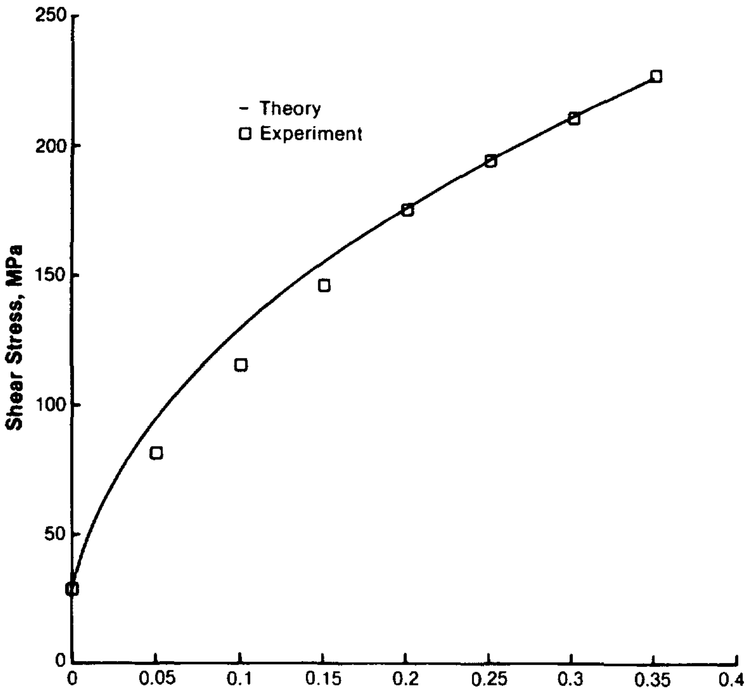

Fig. 6. Shear stress–strain curves of Al-1100.

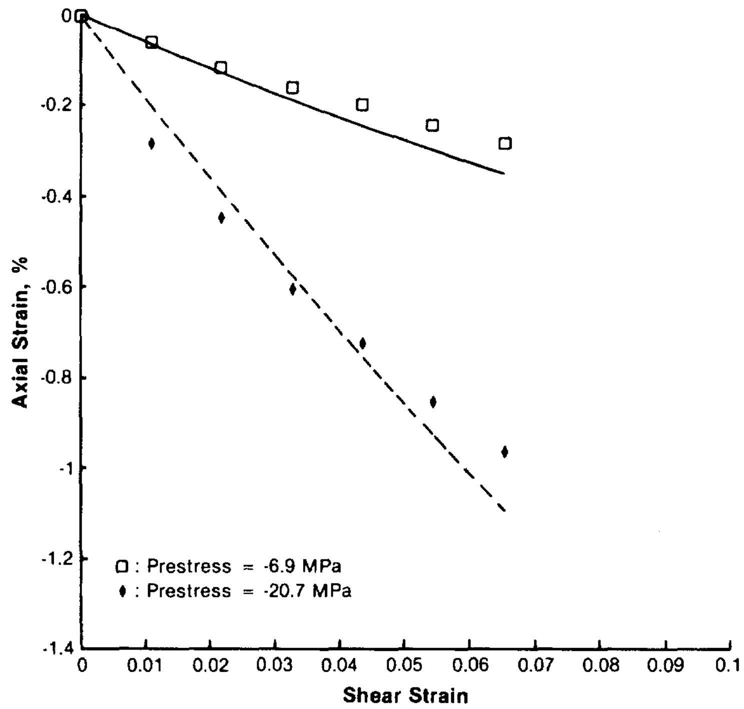

Fig. 7. Axial–shear strain curves with various axial prestresses (Al-1100).

levels have almost the same magnitude, whereas the results of Bailey *et al.* (1972) show that the hoop strain does not increase much with the axial strain at large shear strain levels.

In some published writings such as Canova *et al.* (1984), the rate of hoop strain is assumed to be equal to the rate of radial strain, i.e. $\dot{\varepsilon}_\theta = \dot{\varepsilon}_r$, for thin-walled tubes under tension–torsional loading conditions. This assumption is good only for the axial loading condition. Taylor and Quinney (1932) showed that the hoop strain is not equal to the radial

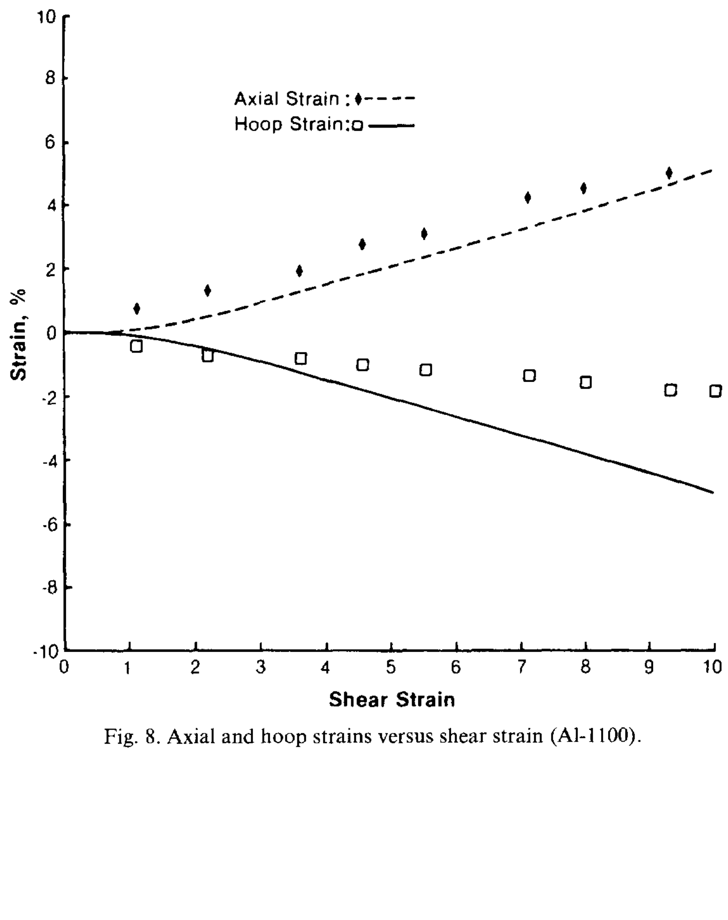

Fig. 8. Axial and hoop strains versus shear strain (Al-1100).

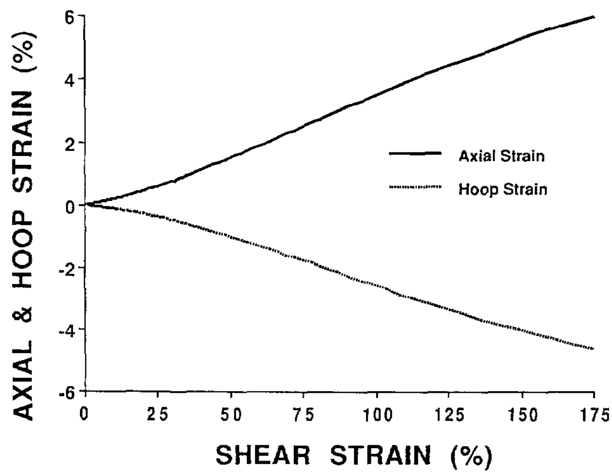

Fig. 9. Experimental axial and hoop strains versus shear strain (high purity Al).

strain under combined tension–torsional loading. In this calculation, we have found that the rate of radial strain is almost zero, i.e. the wall thickness changes very little. And, from eqn (39), the magnitude of the hoop strain is nearly the same as that of the axial strain, in agreement with the experimental observation. We mention that the analysis of Lowe and Lipkin (1990) and Qian and Wu (1994), by use of polycrystal plasticity, also leads to the same trends as predicted by our theory for the axial and hoop strains.

7. CONCLUDING REMARKS

Endochronic constitutive equations have been derived for use in the finite strain range. This has been accomplished by incorporating the concepts of corotational rate, corotational integral and plastic spin into the theory. These equations are then applied to describe torsion of thin-walled tubes subjected to various loading conditions. It has been shown that the oscillatory stress–strain response during monotonic shearing does not arise by use of this set of equations. In addition, the equations successfully describe the torsional behavior under unloading and reloading conditions. Attention has been given to the axial and the hoop strains, and the axial effect during torsional loading. It has been shown that the hoop strain almost has the same magnitude as the axial strain. It has also been shown that the plastic spin has a direct influence on the axial effect during torsion.

REFERENCES

Aifantis, E. C. (1987). The physics of plastic deformation. *Int. J. Plasticity* **3,** 221–247.
Bailey, J. A., Haas, S. L. and Nawab, K. C. (1972). Anisotropy in plastic torsion. *J. Basic Engng* **94,** 231–237.
Canova, G. R., Kocks, U. F. and Jonas, J. J. (1984). Theory of torsion texture development. *Acta Metall.* **32,** 211–226.
Dafalias, Y. F. (1984). The plasticity spin concept and a simple illustration of its role in finite plastic transformations. *Mech. Mater.* **3,** 223–233.
Dafalias, Y. F. (1985a). The plastic spin. *J. Appl. Mech.* **52,** 865–871.
Dafalias, Y. F. (1985b). A missing link in the macroscopic constitutive formulation of large plastic deformation. In *Plasticity Today: Modelling, Methods and Applications* (Edited by A. Sawczuck and G. E. Bianchi), pp. 135–152. Elsevier Applied Science, U.K.
Dafalias, Y. F. (1987). Corotational integral in constitutive formulations. *J. Engng Mech.* **113,** 1967–1973.
Dienes, J. K. (1979). On the analysis of rotation and stress rate in deformation bodies. *Acta Mech.* **32,** 217–232.
Goddard, J. D. and Miller, C. (1966). An inverse for the Jaumann derivative and some applications to the rheology of viscoelastic fluids. *Rheol. Acta* **5,** Heft 3, 177–184.
Green, A. E. and Naghdi, P. M. (1965). A general theory of an elastic-plastic continuum. *Arch. Rat. Anal.* **18,** 251–281.
Hart, E. W. and Chang, Y. W. (1985). Material rotation effects in tension–torsion test: experimental result. In *Plasticity Today* (Edited by A. Sawczuck and G. E. Bianchi), pp. 235–246. Elsevier Applied Science, U.K.
Im, S. and Atluri, S. N. (1987). A study of two finite strain plasticity models: an internal time theory using mandel's director concept and general isotropic/kinematic-hardening theory. *Int. J. Plasticity* **3,** 163–191.
Kratochvil, J. (1973). On a finite strain theory of elastic–inelastic material. *Acta Mech.* **16,** 127–142.

Lee, E. H. (1969). Elastic–plastic deformation at finite strains. *J. Appl. Mech. ASME* **36,** 1–6.

Lee, E. H., Mallet, R. L. and Wertheimer, T. B. (1983). Stress analysis for anisotropic hardening in finite-deformation plasticity. *J. Appl. Mech. ASME* **50,** 554–560.

Lowe, T. C. and Lipkin, J. (1990). Analysis of axial deformation response during reverse shear. Sand90-8417, Sandia National Laboratory.

Mandel, J. (1973). Equations constitutives et directeurs dans les milieux plastiques et viscoplastiques. *Int. J. Solids Structures* **9,** 725–740.

Nagtegaal, J. C. and De Jong, J. E. (1981). Some aspects of non-isotropic workhardening in finite strain plasticity. *Proc. of the Workshop on Plasticity of Metals at Finite Strain: Theory, Experiment and Computation* (Edited by E. H. Lee and R. L. Mallet), pp. 65–102. Stanford University.

Prager, W. (1955). The theory of plasticity: a survey of recent achievements (James Clayton Lecture). *Proc. Inst. Mech. Engrs* **169,** 41.

Qian, Z. and Wu, H. C. (1994). A 2-D texture study based on a double-slip model of polycrystal plasticity with analysis of thin-walled tube under torsion. Submitted for publication to *J. of the Mech. and Phys. of Solids.*

Sowerby, R. and Chu, E. (1984). Rotations stress rates and strain measures in homogeneous deformation processes. *Int. J. Solids Structures* **20,** 1037–1084.

Swift, H. W. (1947). Length change in metal under torsional overstrain. *Engineering* **163,** 253–257.

Taylor, G. I. and Quinney, H. (1932). The plastic distortion of metal. *Phil. Trans. Roy. Soc.* **A230,** 323–362.

Valanis, K. C. (1980). Fundamental consequences of a new intrinsic time measure. plasticity as a limit of the endochronic theory. *Arch. Mech.* **32,** 171–191.

Wang, C. C. (1970). A new representation theory for isotropic function: an answer to professor G. F. Smith's criticism of my paper on representation theory for isotropic function. *Arch. Rat. Mech. Anal.* **36,** 166–223.

White, C. S., Bronkhorst, C. A. and Anand, L. (1990). An improved isotropic kinematic hardening model for moderate deformation metal plasticity. *Mech. Mater.* **10,** 127–147.

Wu, H. C., Lu, J. K. and Pan, W. F. (1994a). Some observations of yield surfaces for 304 stainless steel at large pre-strain. *J. Appl. Mech.* (in press).

Wu, H. C. and Xu, Z. Y. (1989). An extensometer investigation of the axial effect during torsion. In *Proc. Int. Conf. on Constitutive Laws for Eng. Material* (Edited by J. Fan and S. Murakami), pp. 232–238. Chongqing, China.

Wu, H. C. and Xu, Z. (1990). An axial–torsional extensometer for finite deformation. *J. Engng Mater. Tech.* **112,** 330–335.

Wu, H. C., Xu, Z. and Wang, P. T. (1992). The shear stress–strain curve determination from torsion test in the large strain range. *J. Testing and Evaluation ASTM* **20,** 396–402.

Wu, H. C., Xu, Z. and Wang, P. T. (1993). An experimental investigation of torsion at room and elevated temperatures in the large strain range. *Fourth International Symposium on Plasticity and Its Current Applications*, Baltimore, Maryland.

Wu, H. C., Xu, Z. and Wang, P. T. (1994b). Manuscript in preparation.

Wu, H. C. and Yip, M. C. (1981). Endochronic description of cyclic hardening behavior for metallic materials. *J. of Eng. Mater. and Tech. ASME* **103,** 212–217.